



# Anisotropic compact star model: a brief study via embedding

Piyali Bhar<sup>a</sup>

Department of Mathematics, Government General Degree College, Singur, Hooghly, West Bengal 712 409, India

Received: 16 May 2018 / Accepted: 3 February 2019 / Published online: 14 February 2019  
© The Author(s) 2019

**Abstract** In present article a new model of compact star is obtained in the framework of general relativity which does not suffer from any kinds of singularity. We assume that the underlying fluid distribution is anisotropic in nature along with a new form for the metric potential  $e^\lambda$  which is physically reasonable. Though the model parameters depend on four constants  $a$ ,  $b$ ,  $A$  and  $B$  but we have shown that the solutions depend on two free constants since these four constants are correlated to one another. Our proposed model of anisotropic compact star obeys all the necessary physical requirements which have been analyzed with the help of the graphical representation where  $n$  lies in the range of  $-200 \leq n \leq 200$ . We have shown that the model satisfies all the energy conditions as well as the causality condition. The model is potentially stable and also satisfy Harrison–Zeldovich–Novikov’s stability condition.

## 1 Introduction

A well known fact is that the compact objects such as white dwarfs, neutron stars or black hole are formed at the end point of the gravitational collapse of a star when most of their nuclear fuel has been consumed. They are supported by either nuclear or electromagnetic forces which act as an internal pressures, but gravity plays an important role in both the process of the gravitation collapse and in the final equilibrium configuration. The factor which is reasonable behind the type of the ends up object is the star’s mass. White dwarfs are formed from light stars with masses  $M < 4M_\odot$  and radius is  $\sim 10^{-2}R_\odot$ . Moreover it has shown that the maximum allowed mass for white dwarfs is around  $1.4M_\odot$ . [1] ( $M_\odot$ ,  $R_\odot$  are the solar mass and solar radius respectively).

Ruderman [2] was the pioneer who proposed that the pressure inside a highly compact objects shows anisotropic in nature, i.e., it has two components: one is radial pressure  $p_r$

and other one is transverse pressure  $p_t$  orthogonal to the former.  $\Delta = p_t - p_r$  is known as anisotropic factor and  $\frac{2\Delta}{r}$  is anisotropic force which becomes attractive or repulsive according to  $p_r < p_t$  or  $p_r > p_t$ . Bowers and Liang [3], in 1974, wrote a paper on the study of anisotropic distribution of matter which got wide attention. Anisotropy can be revealed due to the existence of solid stellar core or by phase transitions, pion condensation in a star [4], the presence of type-IIIa superfluid [5,6], rotation, electromagnetic field [7–9] etc. The effect of pressure anisotropic has been studied in details in the Refs. [10,11]. By using uniform matter density, anisotropic model has been investigated in [12]. Chan et al. [13] studied the role of the local pressure anisotropy in detail and showed that small anisotropies might in principle drastically change the stability of the system. Some anisotropic compact star models are obtained which admit conformal motion. The solutions depend on the conformal factor and matter density  $\rho$  [14,15] or a relation between radial and transverse pressure etc. [14]. In Ref. [15], a new class of interior solutions for anisotropic stars are obtained by choosing a particular density distribution function of Lorentzian type as provided by Nazari and Mehdipour [16,17] which admits conformal motion in higher dimensional noncommutative spacetime. Some researchers obtained the polytropic quark star model [21] in order to establish a relation between theory and observations. Heintzmann and Hillebrandt [19] described a model of a relativistic, anisotropic neutron star model at high densities by means of several simple assumptions and have shown that for an arbitrary large anisotropy there is no limiting mass for neutron stars, however the maximum mass of a neutron star still lies beyond  $3-4M_\odot$ . Sharma et al. [20] considered the theoretical possibility of anisotropy in strange stars, with densities greater than that of neutron stars but less than that of black holes. Lai and Xu [21] proposed that the polytropic equations of state are stiffer than the conventional realistic models, i.e., the MIT bag model. In the framework of a polytropic model, they show that a very low massive quark star can also exist and be still gravitationally

<sup>a</sup>e-mail: [piyalibhar90@gmail.com](mailto:piyalibhar90@gmail.com)

stable even if the polytropic index  $n > 3$ . The properties of compact stars depends on the assumed description of matter in their interiors. Xu et al. [22] and Azam et al. [23] studied the behavior and the physical properties of several compact objects. A general scheme for compact astrophysical objects which are not composed of neutron matter, but where, given the conditions of very high density in their interiors are presented by Alcock et al. [24] and Haensel et al. [25].

The Randall–Sundrum (RS) second brane-world model [26] is stand on the concept that our 4-dimensional space-time is a hypersurface embedded into the 5-dimensional bulk. After the work done by Randall and Sundrum [26] on brane theory, the study on embedding spacetime attracted the researchers more. If a  $n$ -dimensional space  $V_n$  can be embedded in  $(n+k)$ -dimensional space, where  $k$  is a minimum number of extra dimensions, then  $V_n$  is said to be of embedding class  $k$  of  $n$ -dimensional space. Two very well known important solutions, e.g. Friedmann universe and Schwarzschild’s interior solutions are of class I, (so in this case  $k = 1$ ), on the other hand, Schwarzschild exterior solution is of class II ( $k = 2$ ) and the Kerr metric [27] is of class V ( $k = 5$ ). The Karmarkar condition relates to class one spacetimes. Pandey and Sharma [39] showed that the Karmarkar condition is only a necessary condition for a spacetime to be of class I. A further requirement has to be imposed for sufficiency of the Karmarkar condition. The derivation of the Karmarkar Both charged and uncharged star model of embedding class-I spacetime extensively study in the Refs. [28–38].

We have organized the paper as follows: in Sect. 2 the basic field equations have been discussed, in Sect. 3 we have given a short discussion about embedding class-I spacetime and also obtained a new model. In next section we match our interior space-time with the exterior Schwarzschild line element and junction condition is also discussed. The physical analysis of the model are discussed in Sect. 5. In Sect. 6 we discussed the stability conditions of the present model and some discussions are made in the final section.

## 2 Basic field equations

The interior of a static spherically symmetric spacetime in standard co-ordinate  $x^a = (t, r, \theta, \phi)$  is described by the following line element:

$$ds^2 = e^{v(r)} dt^2 - e^{\lambda(r)} dr^2 - r^2(d\theta^2 + \sin^2 \theta d\phi^2), \quad (1)$$

where  $\lambda$  and  $v$  are the functions of radial coordinate  $r$  only.

The Einstein field equation is,

$$G_{ij} = 8\pi T_{ij}. \quad (2)$$

Here  $G_{ij}$  is the Einstein’s tensor having the following expressions,

$$R_{ij} - \frac{1}{2} R g_{ij} = G_{ij}, \quad (3)$$

where  $R_{ij}$ ,  $R$  and  $g_{ij}$  are the Ricci tensors and Ricci scalar and metric tensor respectively.  $T_{ij}$  is the energy-momentum tensor of the underlying fluid distribution.

Let us assume that the matter involved in the distribution is anisotropic in nature, by using the general expression, we, therefore, get the expression for energy-momentum tensor as follows:

$$T_{\xi}^{\mu} = \rho v^{\mu} v_{\xi} + p_r \chi_{\xi} \chi^{\mu} + p_t (v^{\mu} v_{\xi} - \chi_{\xi} \chi^{\mu} - g_{\xi}^{\mu}), \quad (4)$$

with  $v^{\mu} v_{\xi} = 1 = -\chi_{\xi} \chi^{\mu}$ ,  $\chi_{\xi}$  is the unit space-like vector and  $v^{\mu}$  is the fluid-4 velocity of the rest frame and therefore  $v^{\mu} \chi_{\xi} = 0$ . The above formula gives the components of the energy-momentum tensor of an anisotropic fluid at any point in terms of the density  $\rho$ , the anisotropic and transverse pressures  $p_r$ ,  $p_t$  respectively. With the simple form of line element,  $T_{\xi}^{\mu}$  takes the form:

$$T_0^0 = \rho, T_1^1 = -p_r, T_2^2 = T_3^3 = -p_t, \quad (5)$$

and

$$T_j^k = 0 \text{ if } j \neq k,$$

using (5), for the line element (1), (2) takes the form:

$$8\pi p_r = \frac{e^{-\lambda} - 1}{r^2} + \frac{e^{-\lambda} v'}{r}, \quad (6)$$

$$8\pi p_t = e^{-\lambda} \left( \frac{v''}{2} + \frac{v'^2}{4} - \frac{v' \lambda'}{4} + \frac{v' - \lambda'}{2r} \right), \quad (7)$$

$$8\pi \rho = \frac{1 - e^{-\lambda}}{r^2} + \frac{e^{-\lambda} \lambda'}{r}, \quad (8)$$

where differentiations with respect to  $r$  are denoted by ‘ $'$ ’ and we have chosen  $G = c = 1$ . Here  $G$  is the gravitational constant and  $c$  is the speed of light. The gravitational mass in a sphere of radius ‘ $r$ ’ is given by,

$$m(r) = 4\pi \int_0^r \rho(\omega) \omega^2 d\omega. \quad (9)$$

In next section we shall solve the Eqs.(6)–(8) to obtain the model of compact star.

## 3 A particular model

So form the above field equations (6)–(8), it is noted that we have three field equations for five unknown functions:  $e^v$ ,  $e^{\lambda}$ ,  $\rho$ ,  $p_r$  and  $p_t$ . So to generate a model of compact star, we are free to chose any two of them, though to be a physically realistic model a number of physical conditions to be satisfied by our present model.

To generate a particular model of compact star, let us assume that the co-efficient of  $dr^2$ , i.e.,  $g_{rr}$  has the following form:

$$e^\lambda = 1 + a^2 r^2 (1 + b^5 r^5)^{-n}, \tag{10}$$

where  $a, b$  are some positive constants having the unit  $length^{-1}$  and  $n \in \mathcal{R}$ ,  $\mathcal{R}$  is the set of real numbers. We are the first to use this metric potential.

Now using the relation between the mass function and the metric potential,

$$e^{-\lambda} = 1 - \frac{2m(r)}{r}, \tag{11}$$

the mass function of the star is obtained as,

$$m(r) = \frac{a^2 r^3}{2[a^2 r^2 + (1 + b^5 r^5)^n]}. \tag{12}$$

The metric potential that we use in this paper gives a mass function which is monotonic increasing in nature and regular at the center of the star. At the same time it provides a matter density which gives a profile of monotonic decreasing in nature and gives a finite value at the center of the star. So our chosen metric potential is physically reasonable.

Now for a symmetric tensor  $b_{\mu\nu}$  of a 4-dimensional Riemannian space satisfying the Gauss and Codazzi equations given as

$$R_{\mu\nu\alpha\beta} = \epsilon(b_{\mu\alpha}b_{\nu\beta} - b_{\mu\beta}b_{\nu\alpha}) \tag{13}$$

$$b_{\mu\nu;\alpha} - b_{\mu\alpha;\nu} = 0, \tag{14}$$

can be embedded in 5-dimensional Pseudo-Euclidean space. where ‘(;)’ represents covariant derivatives and  $\epsilon$  takes the value  $-1$  or  $+1$  according to the normal to the manifold being time-like or space-like respectively. For the line element given in (1), the non-zero components of the Riemann curvature tensor are given as,

$$R_{2323} = r^2 \sin^2\theta [1 - e^{-\lambda}]$$

$$R_{1212} = \frac{1}{2} \lambda' r$$

$$R_{1224} = 0$$

$$R_{1414} = e^\nu \left[ \frac{1}{2} v'' + \frac{1}{4} v'^2 - \frac{1}{4} \lambda' v' \right]$$

$$R_{3434} = \frac{r}{2} \sin^2\theta v' e^{\nu-\lambda}.$$

It is clear that the non-zero components of the symmetry tensor  $b_{\mu\nu}$  are  $b_{11}$ ,  $b_{22}$ ,  $b_{33}$ ,  $b_{44}$  and also  $b_{14}(= b_{41})$  due to its symmetry nature and  $b_{33} = b_{22} \sin^2\theta$ . By substituting the components of  $b_{\mu\nu}$  from (13) we get,

$$R_{1414} = \frac{R_{1212}R_{3434} + R_{1224}R_{1334}}{R_{2323}}, \tag{15}$$

with  $R_{2323} \neq 0$  [39]. The space-time that satisfies the condition (15) represents the space time of embedding class I.

For the condition (15), the line element (1) gives the following differential equation

$$\frac{\lambda' v'}{1 - e^\lambda} = -2(v'' + v'^2) + v'^2 + \lambda' v', \tag{16}$$

with  $e^\lambda \neq 1$ . Solving Eq. (16) we get,

$$e^\nu = \left( A + B \int \sqrt{e^\lambda - 1} dr \right)^2, \tag{17}$$

where  $A$  and  $B$  being the constants of integration.

By using (16) and (17), from Eqs. (6) and (7), we obtain the pressure anisotropic  $\Delta = p_t - p_r$  as,

$$8\pi \Delta = \frac{v'}{4e^\lambda} \left[ \frac{2}{r} - \frac{\lambda'}{e^\lambda - 1} \right] \left[ \frac{v'e^\nu}{2rB^2} - 1 \right]. \tag{18}$$

From the Eq. (18), it follows that the anisotropic factor will vanish if the following two case arises:

- Case 1:

$$\frac{\lambda'}{e^\lambda - 1} = \frac{2}{r}, \tag{19}$$

which on integrating gives,

$$e^{-\lambda} = 1 - A_1 r^2, \tag{20}$$

$A_1$  is the constant of integration.

Now using (20), from Eq. (17), we obtain the other metric co-efficient as follows:

$$e^\nu = \left[ A - \frac{B}{\sqrt{A_1}} \sqrt{1 - A_1 r^2} \right]^2. \tag{21}$$

Now using the expression of  $e^\lambda$  in (20), from Eq. (8), we obtain the constant matter density and this solution is nothing but the Schwarzschild’s interior solution [40].

- Case 2:

$$\frac{v'e^\nu}{2rB^2} - 1 = 0,$$

which on integrating, we get,

$$e^\nu = B^2 r^2 + A_2. \tag{22}$$

And like previous case we obtain,

$$e^\lambda = \frac{A_2 + 2B^2 r^2}{A_2 + B^2 r^2}. \tag{23}$$

Where  $A_2$  is the constant of integration.

The solution obtained in (22) and (23) gives, Kohler-Chao solution [41] and it gives non-vanishing Weyl tensor which is suitable for cosmological mode. So we are not interested to consider isotropic pressure.

Substituting the expression for  $e^\lambda$  in (17) and integrating it, the metric coefficient  $e^{\nu(r)}$  becomes,

$$e^\nu = \left[ A + \frac{1}{2} aBr^2\phi_1(r) \right]^2,$$

where

$$\phi_1(r) = \text{hypergeometric } {}_2F_1 \left[ \frac{2}{5}, \frac{n}{2}, \frac{7}{5}, -b^5r^5 \right],$$

and hypergeometric  ${}_2F_1$  is defined as

$$\text{hypergeometric } {}_2F_1(a, b; c; x) = \sum_{k=0}^{\infty} \frac{(a)_k(b)_k}{(c)_k} \frac{x^k}{k!}, \quad (24)$$

where,  $|x| < 1$ ;  $a, b, c$  are real numbers and  $c \neq 0, -1, -2, \dots$ . Here  $(a)_n$  ( $n$  is a positive integer) being Pochhammer symbol defined by,

$$(a)_n = a(a+1) \cdots (a+n-1),$$

with  $(a)_0 = 1$ .

With the help of simple algebra,  $(a)_n$  takes the form,

$$(a)_n = \frac{\Gamma(a+n)}{\Gamma(a)}.$$

Now the series expansion of r.h.s of (24) is,

$$1 + \frac{a \cdot b}{1 \cdot c}x + \frac{a(a+1)b(b+1)}{1 \cdot 2 \cdot c(c+1)}x^2 + \dots$$

Once we have the two metric potentials, by substituting the expressions of metric co-efficient in the field equations (6)–(8), the matter density, radial and transverse pressure becomes,

$$\rho = \frac{a^2 (1 + b^5r^5)^n \{3 + b^5(3 - 5n)r^5\} + a^2(r^2 + b^5r^7)}{8\pi (1 + b^5r^5) \{a^2r^2 + (1 + b^5r^5)^n\}^2} \quad (25)$$

$$p_r = \frac{a}{8\pi} \frac{-2aA + 4B(1 + b^5r^5)^{\frac{n}{2}} - a^2Br^2\phi_1(r)}{\{a^2r^2 + (1 + b^5r^5)^n\} \{2A + aBr^2\phi_1(r)\}} \quad (26)$$

$$p_t = \frac{a(1 + b^5r^5)^{-1+\frac{n}{2}}}{16\pi [a^2r^2 + (1 + b^5r^5)^n]^2 \{2A + aBr^2\phi_1(r)\}} \times \left[ 4a^2Br^2(1 + b^5r^5) - 2B(1 + b^5r^5)^n\phi_2(r) + a(1 + b^5r^5)^{\frac{n}{2}}\phi_3(r) \{2A + aBr^2\phi_1(r)\} \right]. \quad (27)$$

And the anisotropic factor  $\Delta$  is given by,

$$\Delta = \frac{(p_t - p_r)}{1} = \frac{1}{16\pi(1 + b^5r^5) [a^2r^2 + (1 + b^5r^5)^n]^2 \xi(r)} \times \left[ ar^2 \{2a^2(1 + b^5r^5) + 5b^5nr^3(1 + b^5r^5)^n\} \{2aA - 2B(1 + b^5r^5)^{\frac{n}{2}} + a^2Br^2\phi_1(r)\} \right]. \quad (28)$$

Where the expressions for  $\phi_2(r), \phi_3(r), \xi(r)$  are given by,

$$\begin{aligned} \phi_2(r) &= -4 + b^5(-4 + 5n)r^5, \\ \phi_3(r) &= -2 + b^5(-2 + 5n)r^5, \\ \xi(r) &= 2A + aBr^2\phi_1(r). \end{aligned}$$

#### 4 Exterior spacetime and matching conditions

In this section we match our interior spacetime to the Schwarzschild exterior solution

$$ds^2 = \left(1 - \frac{2M}{r}\right) dt^2 - \left(1 - \frac{2M}{r}\right)^{-1} dr^2 - r^2(d\theta^2 + \sin^2\theta d\phi^2), \quad (29)$$

at the boundary  $r = r_\Sigma$ ,  $r_\Sigma$  being the radius of the star and therefore it is obvious that  $r_\Sigma > 2M$ ,  $M$  is the mass of the black hole.

Now for an isotropic fluid sphere at a stellar surface, O'Brien–Synge [42] and Robson [43] proposed a proper junction condition given by,

$$p(r_\Sigma + 0) = p(r_\Sigma - 0), \quad (30)$$

$$g_{ab}(r_\Sigma + 0) = g_{ab}(r_\Sigma - 0), \quad (31)$$

$$\partial_r g_{ab}(r_\Sigma + 0) = \partial_r g_{ab}(r_\Sigma - 0), \quad (32)$$

where  $r_\Sigma$  is the stellar radius,  $p$  is the isotropic pressure,  $g_{ab}$  is the metric components ( $a, b = r, t, \theta, \phi$ ). Now conditions (30) and (32) provide the following relationship,

$$\left(1 - \frac{2m}{r_\Sigma}\right)^{-1} = 1 + a^2r_\Sigma^2(1 + b^5r_\Sigma^5)^{-n}, \quad (33)$$

$$1 - \frac{2m}{r_\Sigma} = \left[ A + \frac{aBr_\Sigma^2\phi(r_\Sigma)}{2} \right]^2, \quad (34)$$

$$\frac{2m}{r_\Sigma^2} = aBr_\Sigma(1 + b^5r_\Sigma^5)^{-\frac{n}{2}} \left[ 2A + aBr_\Sigma^2\phi_1(r_\Sigma) \right], \quad (35)$$

$$\frac{2m}{r_\Sigma^2 \left(1 - \frac{2m}{r_\Sigma}\right)^2} = a^2r_\Sigma(1 + b^5r_\Sigma^5)^{-1-n} \left[ 2 + b^5(2 - 5n)r_\Sigma^5 \right]. \quad (36)$$

Since we are considering the anisotropic fluid sphere the condition given in Eq.(30) changes in our present paper in presence of both radial and tangential pressure. Now  $p_r(r = r_\Sigma) = 0$  gives,

$$-2aA + 4B(1 + b^5r_\Sigma^5)^{\frac{n}{2}} - a^2Br_\Sigma^2\phi_1(r_\Sigma) = 0, \quad (37)$$

but there is a discontinuous tangential pressure. Now to avoid the discontinuity we calculate the surface stresses at the junction boundary by using the Darmois–Israel [44,45] formation.

The expression for surface energy density  $\sigma$  and the surface pressure  $\mathcal{P}$  at the junction surface  $r = r_\Sigma$  are obtained as,

$$\begin{aligned} \sigma &= -\frac{1}{4\pi r_\Sigma} \left[ \sqrt{e^{-\lambda}} \right]_-^+ \\ &= -\frac{1}{4\pi r_\Sigma} \left[ \sqrt{1 - \frac{2m}{r_\Sigma}} - \sqrt{\frac{(1 + b^5 r_\Sigma^5)^n}{a^2 r_\Sigma^2 + (1 + b^5 r_\Sigma^5)^n}} \right], \quad (38) \\ \mathcal{P} &= \frac{1}{8\pi r_\Sigma} \left[ \left\{ 1 + \frac{av'}{2} \right\} \sqrt{e^{-\lambda}} \right]_-^+ \\ &= \frac{1}{8\pi r_\Sigma} \left[ \frac{1 - \frac{m}{r_\Sigma}}{\sqrt{1 - \frac{2m}{r_\Sigma}}} - \frac{1 + \frac{2aBr_\Sigma^2(1+b^5r_\Sigma^5)^{-\frac{n}{2}}}{2A+aBr_\Sigma^2\phi_1(r_\Sigma)}}{\sqrt{1 + a^2r_\Sigma^2(1 + b^5r_\Sigma^5)^{-n}}} \right]. \quad (39) \end{aligned}$$

**5 Physical analysis**

- For our present model,  $e^{\lambda(0)} = 1$  and  $e^{\nu(0)} = A^2$ , a positive constant, and

$$\begin{aligned} (e^\nu)' &= a^2r(1 + b^5r^5)^{-1-n} (2 + b^5(2 - 5n)r^5), \\ (e^\nu)' &= aBr(1 + b^5r^5)^{-\frac{n}{2}} (2A + aBr^2\phi_1(r)). \end{aligned}$$

Clearly  $(e^\nu)'_{r=0} = 0$  and  $(e^\lambda)'_{r=0} = 0$ , indicates that metric co-efficients are regular at the center.

- The central density of the star is given by,

$$8\pi\rho_c = 8\pi\rho(r = 0) = 3a^2 > 0, \quad (40)$$

and density gradient is obtained as,

$$\begin{aligned} 8\pi \frac{d\rho}{dr} &= \frac{1}{(1 + b^5r^5)^2 \{a^2r^2 + (1 + b^5r^5)^n\}^3} \\ &\times \left[ -2a^6r^3(1 + b^5r^5)^2 - 5a^4r(1 + b^5r^5)^n \phi_5(r) \right. \\ &\left. + 5a^2b^5nr^4(1 + b^5r^5)^{2n} \phi_4(r) \right]. \quad (41) \end{aligned}$$

At the point  $r = 0$ ,

$$\frac{d\rho}{dr} = 0; \quad \frac{d^2\rho}{dr^2} = \frac{-10a^4}{\kappa} < 0.$$

- The central pressure of the star is given by,

$$p_c = p_r(r = 0) = p_t(r = 0) = \frac{a}{8\pi} \left( -a + \frac{2B}{A} \right) > 0, \quad (42)$$

and radial and transverse pressure gradients are obtained as,

$$\begin{aligned} 8\pi \frac{dp_r}{dr} &= \frac{ar}{(1 + b^5r^5) \{a^2r^2 + (1 + b^5r^5)^n\}^2} \chi(r) \\ &\times \left[ \{2A + aBr^2\phi_1(r)\} \{2a^2B(1 + b^5r^5)^{\frac{n}{2}}\phi_2(r) \right. \\ &\left. - 10b^5Bnr^3(1 + b^5r^5)^{\frac{3n}{2}}\} + 2a^3(1 + b^5r^5) \right. \\ &\times \{2A - 2Br + aBr^2\phi_1(r)\} \\ &\times \{2(A + Br) + aBr^2\phi_1(r)\} \\ &\left. + a(1 + b^5r^5)^n \phi_6(r) \right] \quad (43) \\ 8\pi \frac{dp_t}{dr} &= \frac{ar}{2(1 + b^5r^5)^2 \{a^2r^2 + (1 + b^5r^5)^n\}^3} \chi(r) \\ &\times \left[ -8a^5r^4(B + b^5Br^5)^2 + 4a(1 + b^5r^5)^{2n} \phi_8(r) \right. \\ &\left. + 10Ab^5Bnr^3(1 + b^5r^5)^{\frac{5n}{2}} \phi_7(r) \right. \\ &\left. + 4a^4ABr^2(1 + b^5r^5)^{1+\frac{n}{2}} \phi_2(r) \right. \\ &\left. - 2a^2AB(1 + b^5r^5)^{\frac{3n}{2}} \phi_9(r) \right. \\ &\left. + 4a^3(1 + b^5r^5)^n \phi_{10}(r) \right. \\ &\left. + a^3B^2r^4(1 + b^5r^5)^n \phi_{11}(r) \psi(r) \right. \\ &\left. + aBr^2(1 + b^5r^5) \phi_{12}(r) g_1(r) \right]. \quad (44) \end{aligned}$$

Where the expressions for  $\chi(r)$ ,  $\phi_i(r)$  ( $i=1,2,\dots,12$ ),  $g_1(r)$ ,  $\psi(r)$  are given by,

$$\begin{aligned} \chi(r) &= \{2A + aBr^2\phi_1(r)\}^2; \\ \phi_4(r) &= \{-8 + b^5(-3 + 5n)r^5\}; \\ \phi_5(r) &= 2 + b^5r^5 \{4 + b^5(2 + 5(-1 + n)n)r^5\} \\ \phi_6(r) &= 20A^2b^5nr^3 - 8B^2(1 + b^5r^5) \\ &\quad + 5ab^5Bnr^5\phi_1(r) \{4A + aBr^2\phi_1(r)\} \\ \phi_7(r) &= -14 + b^5(-4 + 5n)r^5 \\ \phi_8(r) &= 5A^2b^5nr^3 \{7 + b^5(2 - 5n)r^5\} \\ &\quad + B^2(1 + b^5r^5) \{-4 + b^5(-4 + 5n)r^5\} \\ \phi_9(r) &= 24 + b^5r^5(48 - 20n + b^5(24 - 70n + 75n^2)r^5) \\ \phi_{10}(r) &= B^2r^2(1 + b^5r^5) \{-6 + b^5(-6 + 5n)r^5\} \\ &\quad + A^2 \{8 + b^5r^5 \{16 - 5n \\ &\quad + b^5(-4 + 5n)(-2 + 5n)r^5\} \} \\ \phi_{11}(r) &= -5b^5nr^3(1 + b^5r^5)^n \{-7 + b^5(-2 + 5n)r^5\} \\ &\quad + a^2 \{8 + b^5r^5 \{16 - 5n \\ &\quad + b^5(-4 + 5n)(-2 + 5n)r^5\} \} \\ \phi_{12}(r) &= 5b^5Bnr^3(1 + b^5r^5)^{2n} f_7(r) \\ &\quad + 2a^4Br^2(1 + b^5r^5)\phi_2(r) - 20aAb^5nr^3 \\ &\quad \times (1 + b^5r^5)^{\frac{3n}{2}} \{-7 + b^5(-2 + 5n)r^5\} \end{aligned}$$

$$\begin{aligned}
 &+ 4a^3 A(1 + b^5 r^5)^{\frac{n}{2}} \left[ 8 + b^5 r^5 \{16 - 5n\} \right. \\
 &\quad \left. + b^5(-4 + 5n)(-2 + 5n)r^5 \right] \\
 &- a^2 B(1 + b^5 r^5)^n \left[ 24 + b^5 r^5 \{48 - 20n\} \right. \\
 &\quad \left. + b^5(24 - 70n + 75n^2)r^5 \right] \\
 g_1(r) = &\text{hypergeometric } {}_2F_1 \left[ 1, \frac{7}{5} - \frac{n}{2}, \frac{7}{5}, -b^5 r^5 \right] \\
 \psi(r) = &\text{hypergeometric } {}_2F_1 \left[ \frac{2}{5}, \frac{n}{2}, \frac{7}{5}, -b^5 r^5 \right]^2.
 \end{aligned}$$

Now at the point  $r = 0$ ,

- From Eq. (42), we get,

$$\frac{B}{A} > \frac{a}{2}. \tag{45}$$

Again, in the interior of a compact star model, the inequalities  $\rho - p_r \geq 0$ ,  $\rho - p_t \geq 0$  should satisfy what is called the dominant energy condition, proposed by Zeldovich [46]. Therefore, the above two inequalities should hold at the center of the star, which implies,  $\frac{p_c}{\rho_c} \leq 1$ , i.e.,

$$\frac{B}{A} < 2a. \tag{46}$$

Combining the inequalities in (45) and (46), we get a bound for  $\frac{B}{A}$  as,

$$\frac{a}{2} < \frac{B}{A} < 2a. \tag{47}$$

- The equation of state parameters  $\omega_r$  and  $\omega_t$  are obtained as:

$$\omega_r = \frac{p_r}{\rho}; \quad \omega_t = \frac{p_t}{\rho}.$$

- The gravitational redshift is given by,

$$Z = \sqrt{e^{-\nu}} - 1 = \frac{1}{A + \frac{1}{2}aBr^2\phi_1(r)} - 1, \tag{48}$$

and the central redshift is given by,

$$Z_c = \sqrt{e^{-\nu(0)}} - 1 = \frac{1}{A} - 1. \tag{49}$$

Inside the stellar interior this should be non-negative, i.e.,  $\frac{1}{A} - 1 > 0$  implies,  $0 < A < 1$ , this range of constant  $A$  is well satisfied with the numerical values of  $A$  obtained in Table 1.

Now,

$$\frac{dZ}{dr} = -\frac{4aBr(1 + b^5 r^5)^{-\frac{n}{2}}}{[2A + aBr^2\phi_1(r)]^2}, \tag{50}$$

at  $r = 0$ ,

$$\frac{dZ}{dr} = 0, \quad \frac{d^2Z}{dr^2} = -\frac{aB}{A^2} < 0.$$

It shows that the profile of gravitational redshift is a monotonic decreasing function of ‘r’.

- The surface redshift is given by,

$$Z_s = \sqrt{e^{\lambda(r_\Sigma)}} - 1 = \sqrt{1 + a^2 r_\Sigma^2 (1 + b^5 r_\Sigma^5)^{-n}} - 1. \tag{51}$$

In literature, we found that in the absence of a cosmological constant the surface redshift ( $z_s$ ) lies in the range  $z_s \leq 2$  [47–49]. On the other hand, Bohmer and Harko [49] showed that for an anisotropic star in the presence of a cosmological constant the surface redshift obeys the inequality  $z_s \leq 5$ . For our present model, the surface redshift is obtained as 0.5333 and it is interesting to note that the surface redshift of the model do not depend on  $n$ .

- **Energy condition**

The model of an anisotropic compact star will satisfy the all the energy conditions namely, (i) the Null energy condition (NEC), (ii) Weak energy condition (WEC), (iii)

**Table 1** The numerical values of  $a$ ,  $A$ ,  $B$ , central density ( $\rho_c$ ), surface density ( $\rho_s$ ), central pressure ( $p_c$ ) are obtained by fixing  $b = 0.0095$  for a compact star of mass  $M = 1.85M_\odot$  and radius = 9.5

km for different values of  $n$ . The units of  $a$ ,  $A$ ,  $B$ ,  $b$ ,  $\rho_c$ ,  $\rho_s$ ,  $p_c$  are  $\text{km}^{-1}$ ,  $\text{km}^{-2}$ ,  $\text{km}^{-2}$ ,  $\text{km}^{-1}$ ,  $\text{gm} \cdot \text{cm}^{-3}$ ,  $\text{gm} \cdot \text{cm}^{-3}$ ,  $\text{dyne} \cdot \text{cm}^{-2}$  respectively

| $n$    | $a$      | $A$      | $B$       | $\rho_c$                 | $\rho_s$                 | $p_c$                    |
|--------|----------|----------|-----------|--------------------------|--------------------------|--------------------------|
| 5      | 0.122308 | 0.432156 | 0.0398916 | $2.40939 \times 10^{15}$ | $6.32563 \times 10^{14}$ | $3.68233 \times 10^{35}$ |
| 50     | 0.122324 | 0.432127 | 0.0398916 | $2.41004 \times 10^{15}$ | $6.32367 \times 10^{14}$ | $3.6826 \times 10^{35}$  |
| 3000   | 0.12341  | 0.430173 | 0.0398916 | $2.45299 \times 10^{15}$ | $6.19524 \times 10^{14}$ | $3.70055 \times 10^{35}$ |
| – 250  | 0.122215 | 0.432324 | 0.0398916 | $2.40572 \times 10^{15}$ | $6.33673 \times 10^{14}$ | $3.68079 \times 10^{35}$ |
| – 500  | 0.122123 | 0.432489 | 0.0398916 | $2.40212 \times 10^{15}$ | $6.34761 \times 10^{14}$ | $3.67929 \times 10^{35}$ |
| – 2500 | 0.121394 | 0.433801 | 0.0398916 | $2.37353 \times 10^{15}$ | $6.43468 \times 10^{14}$ | $3.66735 \times 10^{35}$ |



Strong energy condition and (iv) Dominant energy conditions if and only if the following inequalities hold:

$$\rho - p_r \geq 0, \rho - p_t \geq 0, \rho - p_r - 2p_t \geq 0. \tag{52}$$

We shall check the above inequalities with the help of graphical representation.

Before going to plot the model parameters of the present model one can note that the expressions of  $e^\lambda$ ,  $e^\nu$ ,  $\rho$ ,  $p_r$ ,  $p_t$  etc. contains four constants  $a$ ,  $b$ ,  $A$  and  $B$ . So first we have to fix some reasonable values to these constants satisfying the Eqs. (33)–(36). For drawing the plots we have consider a compact star of mass  $1.85M_\odot$  and radius = 9.5 km and we fix  $b = 0.0095$ . For these values, by using boundary conditions, we obtain the other constants  $a$ ,  $A$ ,  $B$  for different values of  $n$  which have shown in Table 1.

Using the values of the constant mentioned in the table, the metric potential  $e^\lambda$  and  $e^\nu$  are plotted in Fig. 1(left) and (middle). We can see that both the metric potentials are monotonic increasing function of ‘ $r$ ’. For different values of ‘ $n$ ’, the numerical values of the metric potentials are obtained in table 2. The profile of the matter density  $\rho$  is shown in Fig. 1(right)

which is a monotonic decreasing function of ‘ $r$ ’. For different values of ‘ $n$ ’, the numerical values of the matter density in  $\text{MeV fm}^{-3}$  unit are obtained in table 3. The radial pressure  $p_r$  and transverse pressure  $p_t$  are plotted in Fig. 2(left) and (middle) respectively. Both are monotonic decreasing function of ‘ $r$ ’ and  $p_r(r = r_\Sigma) = 0$  where as  $p_r(r = r_\Sigma) > 0$ . The measure of anisotropy  $\Delta = p_t - p_r$  is plotted in Fig. 2(right). From the graph of  $\Delta$  one can note that  $\Delta > 0$  for  $0 < r \leq r_\Sigma$  and the positive nature of the anisotropic factor helps to construct more compact object which was prosed in [50] because for positive anisotropy offers an repulsive force which helps to hold the model against the collapse. Moreover at the center of the star the anisotropic factor vanishes, i.e.,  $\Delta = 0$  at  $r = 0$ , which is also a necessary condition to construct a compact star model [51, 52]. The equation of state parameters  $\omega_r$  and  $\omega_t$  are plotted in Fig. 3(top) and (bottom) respectively. Both the profiles are monotonic decreasing functions of ‘ $r$ ’ as well as  $0 \leq \omega_r, \omega_t \leq 1$  and it verifies that the underlying fluid distribution is in-exotic in nature [53]. The profile of the mass function and gravitational redshift are shown in Fig. 4(top) and (bottom) respectively. The mass function is monotonic increasing of ‘ $r$ ’ and  $m(r)_{r=0} = 0$  and the gravitational redshift is monotonic decreasing function of

**Table 2** The numerical values of the metric potential  $e^\lambda$  and  $e^\nu$  are obtained by fixing  $b = 0.0095$  for a compact star of mass  $M = 1.85M_\odot$  and radius = 9.5 km for different values of  $n$

| Metric potential | $n$     | $\frac{r}{r_\Sigma} = 0.0$ | $\frac{r}{r_\Sigma} = 0.2$ | $\frac{r}{r_\Sigma} = 0.4$ | $\frac{r}{r_\Sigma} = 0.6$ | $\frac{r}{r_\Sigma} = 0.8$ | $\frac{r}{r_\Sigma} = 1.0$ |
|------------------|---------|----------------------------|----------------------------|----------------------------|----------------------------|----------------------------|----------------------------|
| $e^\lambda$      | 5       | 1                          | 1.054                      | 1.21601                    | 1.48602                    | 1.86404                    | 2.35003                    |
|                  | 50      | 1                          | 1.05402                    | 1.21607                    | 1.48615                    | 1.86419                    | 2.35003                    |
|                  | 3000    | 1                          | 1.05498                    | 1.21988                    | 1.49413                    | 1.87452                    | 2.35003                    |
|                  | – 250   | 1                          | 1.05392                    | 1.21569                    | 1.48534                    | 1.86315                    | 2.35003                    |
|                  | – 500   | 1                          | 1.05384                    | 1.21537                    | 1.48467                    | 1.86228                    | 2.35003                    |
|                  | – 2500  | 1                          | 1.0532                     | 1.21283                    | 1.47935                    | 1.85537                    | 2.35003                    |
|                  | $e^\nu$ | 5                          | 0.186759                   | 0.18676                    | 0.186763                   | 0.186767                   | 0.186774                   |
| 50               |         | 0.186733                   | 0.186734                   | 0.186737                   | 0.186742                   | 0.186748                   | 0.186757                   |
| 3000             |         | 0.185049                   | 0.18505                    | 0.185053                   | 0.185057                   | 0.185064                   | 0.185073                   |
| – 250            |         | 0.186904                   | 0.186905                   | 0.186908                   | 0.186913                   | 0.186919                   | 0.186928                   |
| – 500            |         | 0.187047                   | 0.187047                   | 0.18705                    | 0.187055                   | 0.187061                   | 0.18707                    |
| – 2500           |         | 0.188183                   | 0.188184                   | 0.188187                   | 0.188192                   | 0.188198                   | 0.188207                   |

**Table 3** Matter density  $\rho$  in  $\text{MeV fm}^{-3}$  unit are obtained by fixing  $b = 0.0095$  for a compact star of mass  $M = 1.85M_\odot$  and radius = 9.5 km. for different values of  $n$

| $n$    | $\frac{r}{r_\Sigma} = 0.0$ | $\frac{r}{r_\Sigma} = 0.2$ | $\frac{r}{r_\Sigma} = 0.4$ | $\frac{r}{r_\Sigma} = 0.6$ | $\frac{r}{r_\Sigma} = 0.8$ | $\frac{r}{r_\Sigma} = 1.0$ |
|--------|----------------------------|----------------------------|----------------------------|----------------------------|----------------------------|----------------------------|
| 5      | 1353.59                    | 1353.58                    | 1353.53                    | 1353.46                    | 1353.35                    | 1353.22                    |
| 50     | 1353.96                    | 1353.94                    | 1353.9                     | 1353.82                    | 1353.72                    | 1353.58                    |
| 3000   | 1378.08                    | 1378.07                    | 1378.02                    | 1377.94                    | 1377.84                    | 1377.7                     |
| – 250  | 1351.53                    | 1351.51                    | 1351.47                    | 1351.39                    | 1351.29                    | 1351.15                    |
| – 500  | 1349.5                     | 1349.49                    | 1349.45                    | 1349.37                    | 1349.27                    | 1349.13                    |
| – 2500 | 1333.44                    | 1333.43                    | 1333.38                    | 1333.31                    | 1333.21                    | 1333.08                    |

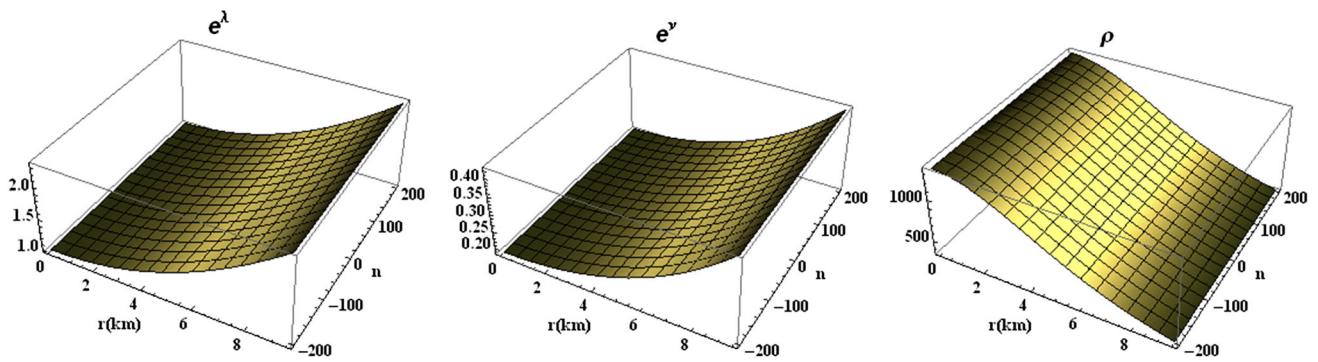


**Fig. 1** (Left) In this figure, along  $x$ -axis,  $y$ -axis and  $z$ -axis we have respectively plotted the radius of the star in km unit, the dimensionless quantity  $n$  which lies in the range  $-200 \leq n \leq 200$  and the metric co-efficient  $e^\lambda$  which is a dimensionless quantity. (middle) along  $x$ -axis,  $y$ -axis and  $z$ -axis we have respectively plotted the radius of the star in km unit, the dimensionless quantity  $n$  which lies in the range  $-200 \leq n \leq 200$  and the metric co-efficient  $e^\nu$  which is a

dimensionless quantity. (Right) Along  $x$ -axis,  $y$ -axis and  $z$ -axis we have respectively plotted the radius of the star in km unit, the dimensionless quantity  $n$  which lies in the range  $-200 \leq n \leq 200$  and the matter density  $\rho$  in  $\text{MeV fm}^{-3}$  unit. All the profiles are drawn for a compact star of mass  $M = 1.85M_\odot$  and radius of the star = 9.5 km. by fixing  $b = 0.0095 \text{ km}^{-1}$

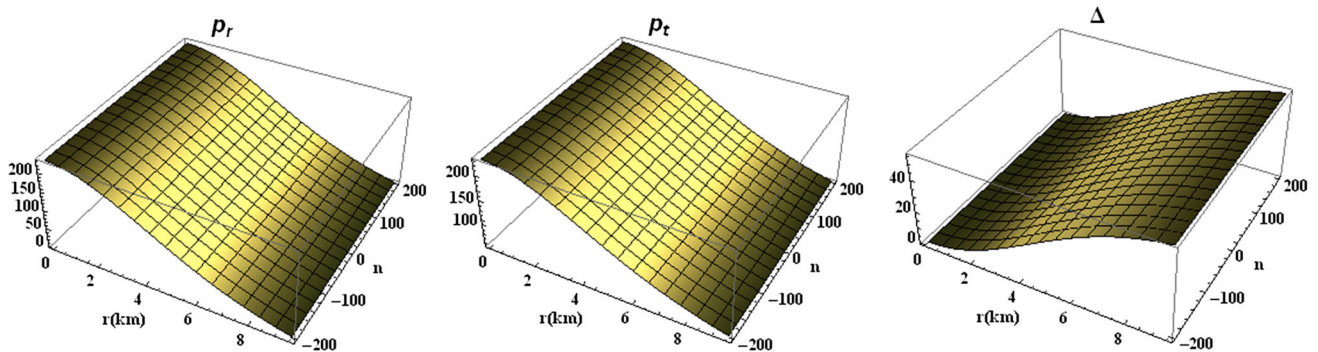


**Fig. 2** (Left) In this figure, along  $x$ -axis,  $y$ -axis and  $z$ -axis we have respectively plotted the radius of the star in km unit, the dimensionless quantity  $n$  which lies in the range  $-200 \leq n \leq 200$  and the radial pressure  $p_r$  in  $\text{MeV fm}^{-3}$  unit. (Middle) along  $x$ -axis,  $y$ -axis and  $z$ -axis we have respectively plotted the radius of the star in km unit, the dimensionless quantity  $n$  which lies in the range  $-200 \leq n \leq 200$  and the

transverse pressure  $p_t$  in  $\text{MeV fm}^{-3}$  unit. (Right) along  $x$ -axis,  $y$ -axis and  $z$ -axis we have respectively plotted the radius of the star in km unit, the dimensionless quantity  $n$  which lies in the range  $-200 \leq n \leq 200$  and the anisotropic factor  $\Delta$  in  $\text{MeV fm}^{-3}$  unit. All the profiles are drawn for a compact star of mass  $M = 1.85M_\odot$  and radius of the star = 9.5 km. by fixing  $b = 0.0095 \text{ km}^{-1}$

‘ $r$ ’. However Buchdahl [54] gave a clear predictions about the maximum possible mass of relativistic stars in the form of the limit  $M < \frac{4R}{9}$ . For our present model the ratio of  $\frac{M}{R}$  is obtained as 0.287 lies in the range proposed by Buchdahl [54]. The profiles of  $\rho - p_r$ ,  $\rho - p_t$ ,  $\rho - p_r - 2p_t$  are shown in Fig. 5 and it verifies that all the inequalities stated in Eq. (52) are holds and consequently our model satisfies all the energy conditions.

may consult [56].)  $\rho_c$  is the central density of the star whose expression has given in (40) and  $M = m(r = r_\Sigma)$ . For our present model the expression is obtained as,

$$\frac{\partial M}{\partial \rho_c} = \frac{4\pi r_\Sigma^3 (1 + b^5 r_\Sigma^5)^{-n}}{3 \left(1 + \frac{8}{3} \rho_c \pi r_\Sigma^2 (1 + b^5 r_\Sigma^5)^{-n}\right)^2}. \tag{53}$$

With the help of the graphical representation, in Fig. 6, we have shown that the above inequality is satisfied by our present model.

## 6 Stability

### 6.1 The static stability criterion due to Harrison–Zeldovich–Novikov

Based on the work done by Harrison *et al.* [55] and Zeldovich–Novikov [46], for a star to be stable, it has to satisfy the inequality  $\frac{\partial M}{\partial \rho_c} > 0$  (for a details discussion one

### 6.2 Causality condition and method of cracking

For any relativistic anisotropic stellar model, some basic physical conditions should be satisfied, some of them have been discussed in the previous section. One of the most important properties among the physical conditions is the causality condition, i.e., the radial and transverse veloc-



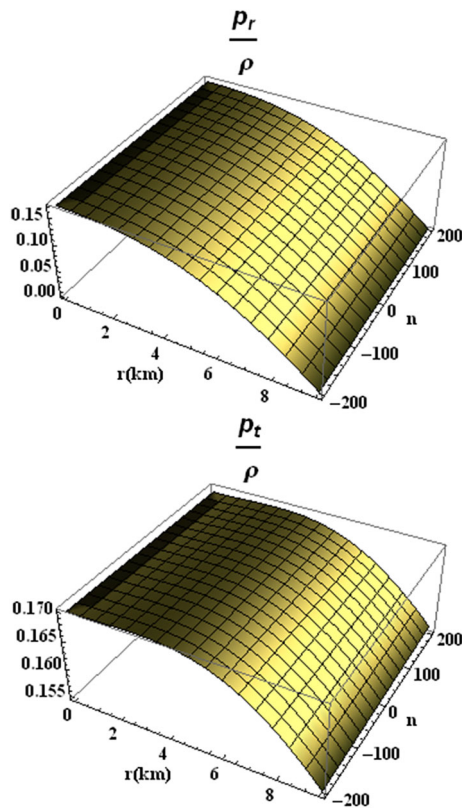


**Fig. 3** (Top) In this figure, along  $x$ -axis,  $y$ -axis and  $z$ -axis we have respectively plotted the radius of the star in km unit, the dimensionless quantity  $n$  which lies in the range  $-200 \leq n \leq 200$  and the ratio of radial pressure  $p_r$  to the matter density  $\rho$  which is a dimensionless quantity. (bottom) along  $x$ -axis,  $y$ -axis and  $z$ -axis we have respectively plotted the radius of the star in km unit, the dimensionless quantity  $n$  which lies in the range  $-200 \leq n \leq 200$  and the ratio of transverse pressure  $p_t$  to the matter density  $\rho$  which is a dimensionless quantity. Both the profiles are drawn for a compact star of mass  $M = 1.85M_\odot$  and radius of the star = 9.5 km by fixing  $b = 0.0095 \text{ km}^{-1}$

ity of sound should not exceed the speed of the light, i.e.,  $v_r^2, v_t^2 \leq 1$  [57,58]. At the same time, Le Chatelier’s principle requires that speed of sound must be positive i.e.,  $v_r^2, v_t^2 > 0$ . Using the above two inequalities one gets,  $0 < v_r^2, v_t^2 \leq 1$ .

Where  $v_r^2$  and  $v_t^2$  are defined as,

$$v_r^2 = \frac{dp_r}{d\rho} = \frac{p'_r}{\rho'} \tag{54}$$

$$v_t^2 = \frac{dp_t}{d\rho} = \frac{p'_t}{\rho'} \tag{55}$$

In the Eqs.(54) and (55) ‘ $\prime$ ’ denotes differentiation with respect to ‘ $r$ ’ and the expressions of  $\rho'$ ,  $p'_r$ ,  $p'_t$  are obtained in Eqs.(41)–(44). The causality condition is well verified by the Fig. 7(left) and (middle).

Based on the radial and transverse velocity of sound, in 1992, Herrera [57] proposed a rule which state if the tangential speed of pressure wave  $v_t$  is larger than the radial speed

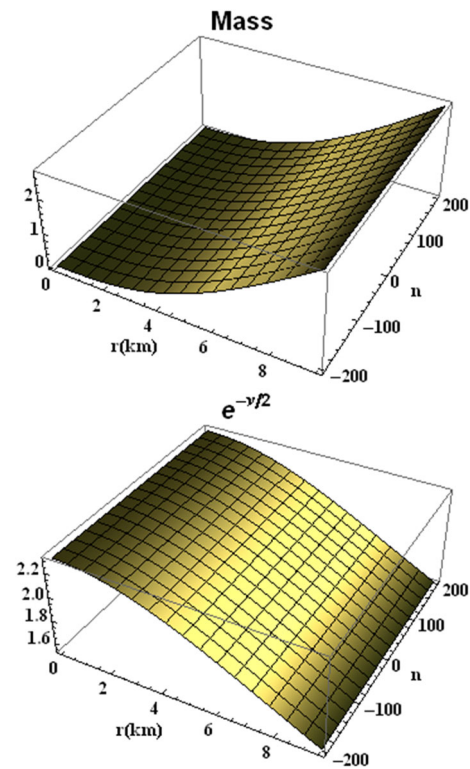


**Fig. 4** (Top) Along  $x$ -axis,  $y$ -axis and  $z$ -axis we have respectively plotted the radius of the star in km unit, the dimensionless quantity  $n$  which lies in the range  $-200 \leq n \leq 200$  and mass of the star in km unit. (Bottom) Along  $x$ -axis,  $y$ -axis and  $z$ -axis we have respectively plotted the radius of the star in km unit, the dimensionless quantity  $n$  which lies in the range  $-200 \leq n \leq 200$  and the gravitational redshift which is also a dimensionless quantity. Both the profiles are drawn for a compact star of mass  $M = 1.85M_\odot$  and radius of the star = 9.5 km by fixing  $b = 0.0095 \text{ km}^{-1}$

of pressure waves  $v_r$  then the model is potentially stable and this fact is known as “cracking method” and mathematically it implies  $v_t^2 - v_r^2 < 0$  is needed throughout the interior of the stellar configuration for star’s stability. Since we are dealing here very complicated expression for  $v_r$  and  $v_t$ , it is not possible for us to check this inequality by analytically rather to check the inequality, we have drawn the profile of  $v_t^2 - v_r^2$  in Fig. 7(right).

Now at the center of the star, the expressions for  $v_r^2$  and  $v_t^2$  are obtained as,

$$v_{r0}^2 = \frac{-a^2 A^2 + 2aAB + B^2}{5a^2 A^2}; \quad v_{t0}^2 = \frac{-2a^2 A^2 + 3aAB + B^2}{5a^2 A^2}$$

$$v_{t0}^2 - v_{r0}^2 = \frac{aAB - a^2 A^2}{5a^2 A^2} < 0 \Rightarrow \frac{B}{A} < a.$$

The above inequality refines the range of  $\frac{B}{A}$  in Eq. (47) as,

$$\frac{a}{2} < \frac{B}{A} < a.$$

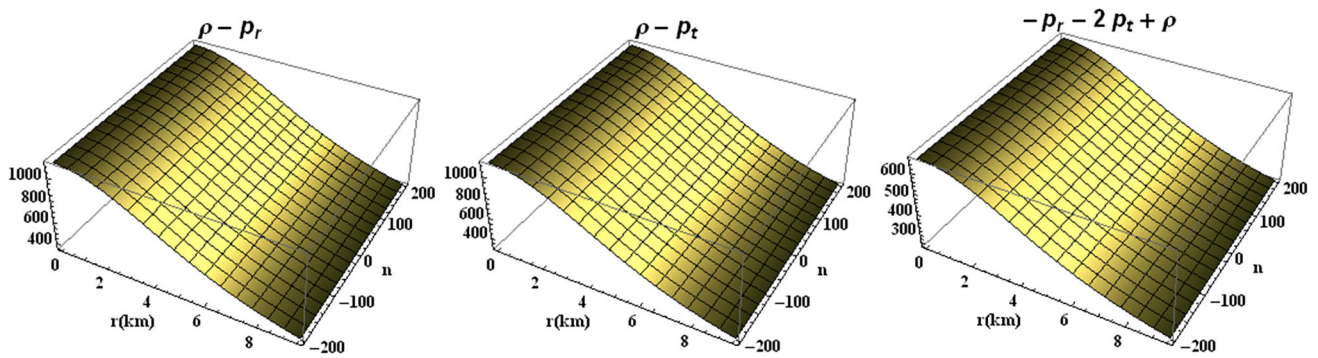


**Fig. 5** (Left) In this figure, along  $x$ -axis,  $y$ -axis and  $z$ -axis we have respectively plotted the radius of the star in km unit, the dimensionless quantity  $n$  which lies in the range  $-200 \leq n \leq 200$  and  $\rho - p_r$  in  $\text{MeV fm}^{-3}$  unit. (Middle) Along  $x$ -axis,  $y$ -axis and  $z$ -axis we have respectively plotted the radius of the star in km unit, the dimensionless quantity  $n$  which lies in the range  $-200 \leq n \leq 200$  and  $\rho - p_t$

in  $\text{MeV fm}^{-3}$  unit. (Right) Along  $x$ -axis,  $y$ -axis and  $z$ -axis we have respectively plotted the radius of the star in km unit, the dimensionless quantity  $n$  which lies in the range  $-200 \leq n \leq 200$  and  $\rho - p_r - 2p_t$  in  $\text{MeV fm}^{-3}$  unit. All the profiles are drawn for a compact star of mass  $M = 1.85M_\odot$  and radius of the star  $= 9.5 \text{ k}$ . by fixing  $b = 0.0095 \text{ km}^{-1}$

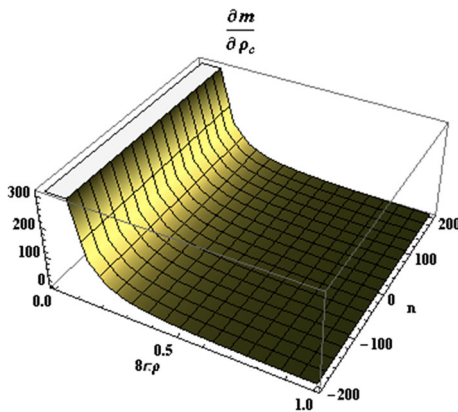


**Fig. 6** In this figure, along  $x$ -axis,  $y$ -axis and  $z$ -axis we have respectively plotted the matter density  $\rho$  in  $\text{MeV fm}^{-3}$  unit, the dimensionless quantity  $n$  which lies in the range  $-200 \leq n \leq 200$  and  $\frac{\partial M}{\partial \rho_c}$ . The profile is drawn for a compact star of mass  $M = 1.85M_\odot$  and radius of the star  $= 9.5 \text{ km}$ . by fixing  $b = 0.0095 \text{ km}^{-1}$

values of  $\Gamma_r, \Gamma_t$  are obtained in Table 4. We note that both  $\Gamma_r, \Gamma_t > \frac{4}{3}$  everywhere inside the anisotropic stellar model for all values of  $n$ .

### 7 Discussion

In our present paper, a new model of compact star has been obtained by assuming the underlying fluid distribution is anisotropic in nature. The model is obtained by solving the Einstein’s field equations which contains three non linear ordinary differential equations with five unknown functions  $(\rho, p_r, p_t, e^\lambda, e^\nu)$ . So to solve the equations one have to choose any two of them and by our knowledge of algebra we can do it in  $5C_2 = 10$  different ways. If one choose Krori–Barua *ansatz* [60], both  $e^\lambda$  and  $e^\nu$  are known functions of ‘ $r$ ’ and by choosing this *ansatz* one need not solve any differential equations to model a compact star rather one has to just replace the expressions for the metric co-efficients and has to perform some algebraic calculations. In literature several number of papers have done by choosing KB *ansatz* [53,61–68]. Some compact star models are developed by choosing metric co-efficients  $e^\lambda$  along with a reasonable equation of state (relation between the matter density  $\rho$  and radial pressure  $p_r$ ) [69–74], by choosing  $e^\lambda$  along with  $p_r$  [75–77].

In present paper we obtain a new class of compact star model in embedding class one spacetime. The study has been done by choosing a new expression for  $e^\lambda$  and the reason of adopting such an metric potential has been discussed earlier. Since our spacetime satisfy the Karmakar’s condition the other metric co-efficient has been obtained very easily from a well known relation, as in case of embedding class-I spacetime the two metric co-efficients are related to each other by a differential equation. So this model has been obtained

### 6.3 Adiabatic index

The adiabatic index  $\Gamma$  for an isotropic fluid sphere was proposed by Chan *et al.* [13] given by,

$$\Gamma = \frac{\rho + p}{p} \frac{dp}{d\rho}, \tag{56}$$

and the above definition for anisotropic fluid sphere changes as,

$$\Gamma_r = \frac{\rho + p_r}{p_r} \frac{dp_r}{d\rho} \quad \text{and} \quad \Gamma_t = \frac{\rho + p_t}{p_t} \frac{dp_t}{d\rho}. \tag{57}$$

Bondi [59] proposed that,  $\Gamma > 4/3$ , is the condition for the stability of a Newtonian sphere and  $\Gamma = 4/3$  being the condition for a neutral equilibrium. The profile of the adiabatic index  $\Gamma_r$  and  $\Gamma_t$  are shown in Fig. 8 and the numerical

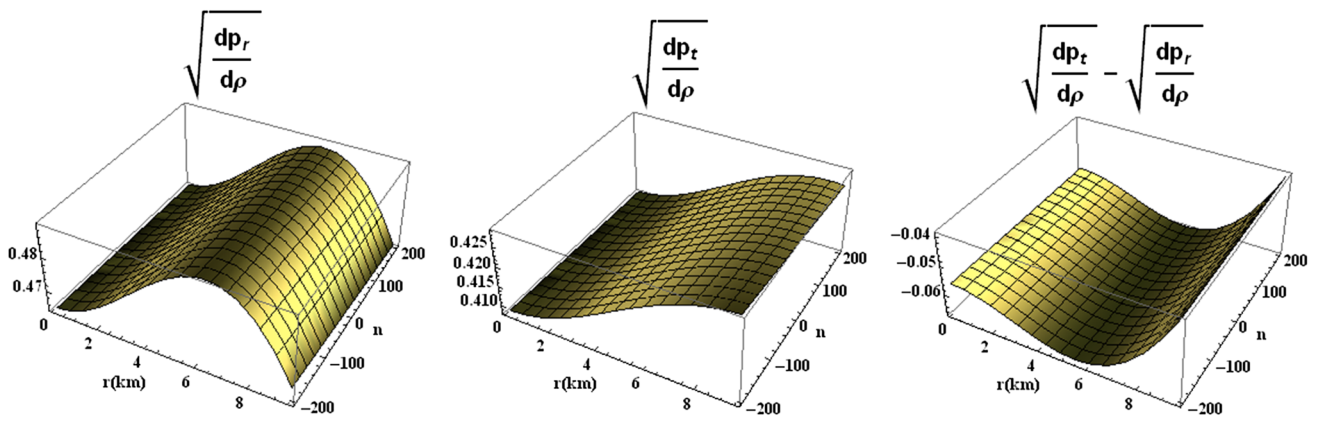


**Fig. 7** (Left) Along  $x$ -axis,  $y$ -axis and  $z$ -axis we have respectively plotted the radius of the star in km unit, the dimensionless quantity  $n$  which lies in the range  $-200 \leq n \leq 200$  and the radial velocity of sound  $\sqrt{\frac{dp_r}{d\rho}}$  which is a dimensionless quantity. (Middle) Along  $x$ -axis,  $y$ -axis and  $z$ -axis we have respectively plotted the radius of the star in km unit, the dimensionless quantity  $n$  which lies in the range  $-200 \leq n \leq 200$  and the transverse velocity of sound  $\sqrt{\frac{dp_t}{d\rho}}$  which is a

dimensionless quantity. (Right) Along  $x$ -axis,  $y$ -axis and  $z$ -axis we have respectively plotted the radius of the star in km unit, the dimensionless quantity  $n$  which lies in the range  $-200 \leq n \leq 200$  and the difference between transverse and radial velocity of sound  $\sqrt{\frac{dp_t}{d\rho}} - \sqrt{\frac{dp_r}{d\rho}}$  which is a dimensionless quantity. All the profiles are drawn for a compact star of mass  $M = 1.85M_\odot$  and radius of the star = 9.5 km by fixing  $b = 0.0095 \text{ km}^{-1}$

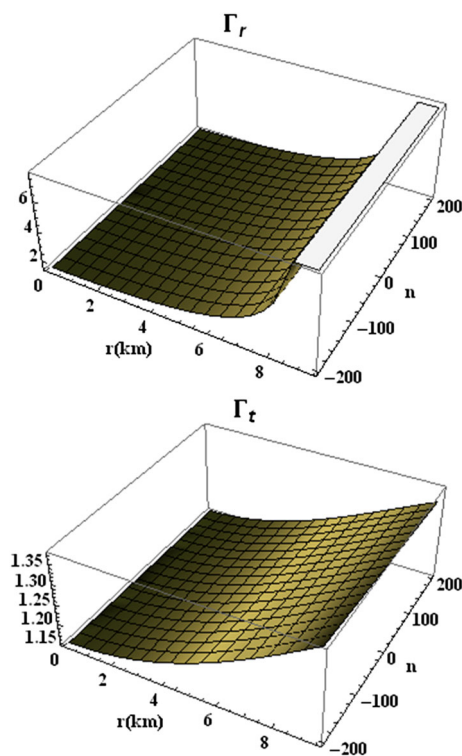


**Fig. 8** (Top) In this figure, along  $x$ -axis,  $y$ -axis and  $z$ -axis we have respectively plotted the radius of the star in km unit, the dimensionless quantity  $n$  which lies in the range  $-200 \leq n \leq 200$  and the radial adiabatic index  $\Gamma_r$  which is a dimensionless quantity. (Bottom) Along  $x$ -axis,  $y$ -axis and  $z$ -axis we have respectively plotted the radius of the star in km unit, the dimensionless quantity  $n$  which lies in the range  $-200 \leq n \leq 200$  and the transverse adiabatic index  $\Gamma_t$  which is a dimensionless quantity. Both the profiles are drawn for a compact star of mass  $M = 1.85M_\odot$  and radius of the star = 9.5 km by fixing  $b = 0.0095 \text{ km}^{-1}$

without assuming any equation of state (a relation between the matter density and the pressure). But we have shown the relation between the pressure and density through graphical representation in Fig. 9. Figure 9 shows that  $p_r$  vs.  $\rho$  and  $p_t$  vs.  $\rho$  follow almost linear equation of state. The value of the constant  $a$  and both central density  $\rho_c$  and central pressure  $p_c$  increase as  $n$  increases on the contrary the values of the integrating constant  $A$  decreases as  $n$  increases and  $B$  remains unchanged for all values of  $n$ .

In 2008, Herrera et al. [79] proposed an algorithm to obtain static spherically symmetric anisotropic solutions of Einstein’s field equations and they showed that this solution can be generated from EFEs by two generating functions  $\zeta(r)$ ,  $\Pi(r)$  given as,

$$e^{\nu(r)} = \exp \int \left[ \left( 2\zeta(r) - \frac{2}{r} \right) dr \right], \tag{58}$$

$$\Pi(r) = p_r - p_t. \tag{59}$$

For our present model, these two generating functions are obtained as,

$$\zeta(r) = \frac{1}{r} + \frac{2aBr(1 + b^5r^5)^{-\frac{n}{2}}}{2A + aBr^2\phi_1(r)} \tag{60}$$

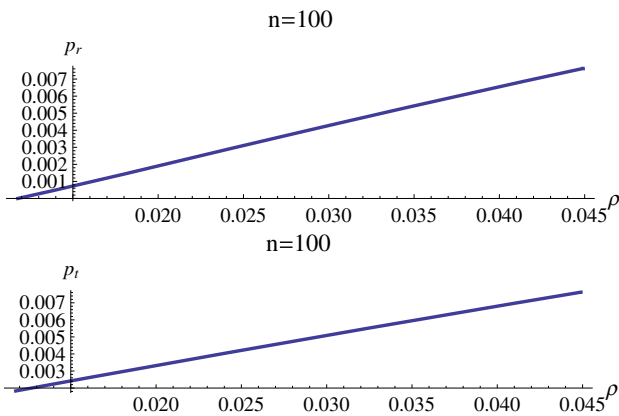
$$\Pi(r) = -\Delta. \tag{61}$$

The most important characteristic of the present study is that all the results have been discussed through 3- dimensional analysis when  $-200 \leq n \leq 200$ . Similar plot can be drawn for  $n > 200$  as well as  $n < -200$ .



**Table 4** The numerical values of  $\Gamma_r$  and  $\Gamma_t$  are obtained by fixing  $b = 0.0095$  for a compact star of mass  $M = 1.85M_\odot$  and radius  $= 9.5$  km. for different values of  $n$ 

| Adiabatic index | $n$   | $\frac{r}{r_\Sigma} = 0.0$ | $\frac{r}{r_\Sigma} = 0.2$ | $\frac{r}{r_\Sigma} = 0.4$ | $\frac{r}{r_\Sigma} = 0.6$ | $\frac{r}{r_\Sigma} = 0.8$ | $\frac{r}{r_\Sigma} = 1.0$ |
|-----------------|-------|----------------------------|----------------------------|----------------------------|----------------------------|----------------------------|----------------------------|
| $\Gamma_r$      | 5     | 1.48667                    | 1.48667                    | 1.4867                     | 1.48674                    | 1.48679                    | 1.48686                    |
|                 | 50    | 1.48667                    | 1.48668                    | 1.4867                     | 1.48674                    | 1.4868                     | 1.48687                    |
|                 | 3000  | 1.48722                    | 1.48723                    | 1.48726                    | 1.4873                     | 1.48735                    | 1.48742                    |
|                 | -250  | 1.48662                    | 1.48663                    | 1.48665                    | 1.48669                    | 1.48675                    | 1.48682                    |
|                 | -500  | 1.48658                    | 1.48659                    | 1.48661                    | 1.48665                    | 1.4867                     | 1.48677                    |
|                 | -2500 | 1.48627                    | 1.48628                    | 1.4863                     | 1.48634                    | 1.48639                    | 1.48646                    |
| $\Gamma_t$      | 5     | 1.14873                    | 1.14873                    | 1.14873                    | 1.14874                    | 1.14875                    | 1.14876                    |
|                 | 50    | 1.14861                    | 1.14861                    | 1.14862                    | 1.14862                    | 1.14863                    | 1.14864                    |
|                 | 3000  | 1.14093                    | 1.14093                    | 1.14093                    | 1.14094                    | 1.14095                    | 1.14096                    |
|                 | -250  | 1.14939                    | 1.1494                     | 1.1494                     | 1.14941                    | 1.14941                    | 1.14943                    |
|                 | -500  | 1.15005                    | 1.15005                    | 1.15005                    | 1.15006                    | 1.15007                    | 1.15008                    |
|                 | -2500 | 1.15529                    | 1.15529                    | 1.1553                     | 1.1553                     | 1.15531                    | 1.15532                    |

**Fig. 9** In this figure we have shown the variation of the radial and transverse pressure with respect to the matter density. (Top) Along  $x$ -axis and  $y$ -axis we have respectively plotted the matter density  $\rho$  in  $\text{MeV fm}^{-3}$  unit and radial pressure  $p_r$  in  $\text{MeV fm}^{-3}$  unit. (Bottom) Along  $x$ -axis and  $y$ -axis we have respectively plotted the matter density  $\rho$  in  $\text{MeV fm}^{-3}$  unit and transverse pressure  $p_t$  in  $\text{MeV fm}^{-3}$  unit. Both the profiles are drawn for a compact star of mass  $M = 1.85M_\odot$  and radius of the star  $= 9.5$  km by fixing  $b = 0.0095 \text{ km}^{-1}$ . Both the figures are drawn for  $n = 100$ 

**Data Availability Statement** This manuscript has no associated data or the data will not be deposited. [Authors' comment: There is no data.]

**Open Access** This article is distributed under the terms of the Creative Commons Attribution 4.0 International License (<http://creativecommons.org/licenses/by/4.0/>), which permits unrestricted use, distribution, and reproduction in any medium, provided you give appropriate credit to the original author(s) and the source, provide a link to the Creative Commons license, and indicate if changes were made. Funded by SCOAP<sup>3</sup>.

## References

1. S.L. Shapiro, S.A. Teukolsky, *Black Holes, White Dwarfs and Neutron Stars: The Physics of Compact Objects* (Cornell University, Ithaca, 1983)
2. M. Ruderman, *Annu. Rev. Astron. Astrophys.* **10**, 427–476 (1972)
3. R.L. Bowers, E.P.T. Liang, *Astrophys. J.* **188**, 657 (1974)
4. R.F. Sawyer, *Phys. Rev. Lett.* **29**(6), 382–385 (1972)
5. R. Kippenhahn, A. Weigert, *Stellar Structure and Evolution* (Springer, New York, 1990)
6. A.I. Sokolov, *Sov. Phys. JETP* **52**(4), 575–576 (1980)
7. A. Putney, *ApJL* **451**, L67 (1995)
8. D. Reimers, S. Jordan, D. Koester, N. Bade, T. Kohler, L. Wisotzki, *Astron. Astrophys.* **311**, 572–578 (1996)
9. A.P. Martinez, R.G. Felipe, D.M. Paret, *Int. J. Mod. Phys. D* **19**, 1511 (2010)
10. L. Herrera, N.O. Santos, *Phys. Rep.* **286**, 53 (1997)
11. L. Herrera, A. Di Prisco, J. Martin, J. Ospino, N.O. Santos, O. Troconis, *Phys. Rev. D* **69**, 084026 (2004)
12. S.D. Maharaj, R. Maartens, *Gen. Relativ. Gravit.* **21**(9), 899–905 (1989)
13. R. Chan, L. Herrera, N.O. Santos, *Mon. Not. R. Astron. Soc.* **265**, 533 (1993)
14. F. Rahaman, M. Jamil, R. Sharma, K. Chakraborty, *Astrophys. Space Sci.* **330**, 249 (2010)
15. P. Bhar, F. Rahaman, S. Ray, V. Chatterjee, *Eur. Phys. J. C* **75**, 190 (2015)
16. K. Nozari, S.H. Mehdipour, *JHEP* **0903**, 061 (2009)
17. S.H. Mehdipour, *Eur. Phys. J. Plus* **127**, 80 (2012)
18. S. Thirukkanesh, F.C. Ragel, *Pramana J. Phys.* **78**, 687 (2012)
19. H. Heintzmann, W. Hillebrandt, *Astron. Astrophys.* **38**, 51 (1975)
20. R. Sharma et al., *Gen. Relativ. Gravit.* **33**, 999 (2001)
21. X.Y. Lai, R.X. Xu, *Astropart. Phys.* **31**, 128 (2009)
22. R.X. Xu et al., *Chin. Phys. Lett.* **18**, 837 (2001)
23. M. Azam et al., *Chin. Phys. Lett.* **33**, 070401 (2016)
24. C. Alcock et al., *Astrophys. J.* **310**, 261 (1986)
25. P. Haensel et al., *Astron. Astrophys.* **160**, 121 (1986)

26. L. Randall, R. Sundrum, *Phys. Rev. Lett.* **83**, 3370 (1999)
27. R.P. Kerr, *Phys. Rev. Lett.* **11**, 237 (1963)
28. P. Bhar, K.N. Singh, N. Sarkar, F. Rahaman, *Eur. Phys. J. C* **77**, 596 (2017)
29. P. Bhar, *Eur. Phys. J. Plus* **132**, 274 (2017)
30. P. Bhar, K.N. Singh, F. Rahaman, N. Pant, S. Banerjee, *Int. J. Mod. Phys. D* **26**, 1750078 (2017)
31. P. Bhar, S.K. Maurya, Y.K. Gupta, T. Manna, *Eur. Phys. J. A* **52**, 312 (2016)
32. K.N. Singh, P. Bhar, N. Pant, *Int. J. Mod. Phys. D* **25**(11), 1650099 (2016)
33. P. Bhar, K.N. Singh, T. Manna, *Int. J. Mod. Phys. D* **26**, 1750090 (2017)
34. P. Bhar, M. Govender, *Int. J. Mod. Phys. D* **26**, 1750053 (2017)
35. K.N. Singh, P. Bhar, F. Rahaman, N. Pant, M. Rahaman, *Mod. Phys. Lett. A* **32**, 1750093 (2017)
36. K.N. Singh, P. Bhar, N. Pant, *Astrophys. Space Sci.* **361**, 339 (2016)
37. S. Thakadiyil, M.K. Jasim, *Int. J. Theor. Phys.* **52**, 3960 (2013)
38. K.N. Singh, N. Pant, N. Pradhan, *Astrophys. Space Sci.* **361**, 173 (2016)
39. S.N. Pandey, S.P. Sharma, *Gen. Relativ. Gravit.* **14**, 113 (1981)
40. K. Schwarzschild, *Sitz. Deut. Akad. Wiss. Math. Phys. Berlin* **24**, 424 (1916) [**Schw Int**]
41. M. Kohler, K.L. Chao, *Z. Naturforschg* **20**, 1537 (1965)
42. S. O'Brien, J.L. Synge, *Jump Conditions at Discontinuities in General Relativity*, in *Communications of the Dublin Institute for Advanced Studies*, Dublin (1952)
43. E.H. Robson, *Ann. Inst. Henri Poincare* **16**, 41 (1972)
44. W. Israel, *Nuovo Cimento B* **44**, 48 (1966)
45. W. Israel, *Nuovo Cimento B* **48**, 463 (1967) (**Erratum**)
46. Y.B. Zeldovich, I.D. Navikov, *Relativistic Astrophysics, vol 1, Stars and Relativity* (University of Chicago Press, Chicago, 1971)
47. H.A. Buchdahl, *Phys. Rev.* **116**, 1027 (1959)
48. N. Straumann, *General Relativity and Relativistic Astrophysics* (Springer, Berlin, 1984)
49. C.G. Böhrmer, T. Harko, *Class. Quantum Gravity* **23**, 6479 (2006)
50. M.K. Gokhroo, A.L. Mehra, *Gen. Relativ. Gravit.* **26**, 75 (1994)
51. B.V. Ivanov, *Phys. Rev. D* **65**, 104011 (2002)
52. R.L. Bowers, E.P.T. Liang, *Astrophys. J.* **188**, 657 (1974)
53. F. Rahaman et al., *Phys. Rev. D* **82**, 104055 (2010)
54. H.A. Buchdahl, *Phys. Rev. D* **116**, 1027 (1959)
55. B.K. Harrison, K.S. Thorne, M. Wakano, J.A. Wheeler, *Gravitation Theory and Gravitational Collapse* (1965)
56. P. Haensel, A.Y. Potekin, D.G. Yakovlev, *Neutron Stars 1: Equation of State and Structure*, vol. 1 (Springer, Berlin, 2007)
57. L. Herrera, *Phys. Lett. A* **165**, 206 (1992)
58. H. Abreu, H. Hernandez, L.A. Nunes, *Class. Quantum Gravity* **24**, 4631 (2007)
59. H. Bondi, *Proc. R. Soc. Lond. A* **281**, 39 (1964)
60. K.D. Krori, J. Barua, *J. Phys. A Math. Gen.* **8**, 508 (1975)
61. P. Bhar, F. Rahaman, A. Jawad, S. Islam, *Astrophys. Space Sci.* **360**, 32 (2015)
62. P. Bhar, *Astrophys. Space Sci.* **357**, 46 (2015)
63. P. Bhar, *Astrophys. Space Sci.* **356**, 365–373 (2015)
64. P. Bhar, *Astrophys. Space Sci.* **356**, 309–318 (2015)
65. V. Varela, F. Rahaman, S. Ray, K. Chakraborty, M. Kalam, *Phys. Rev. D* **82**, 044052 (2010)
66. P. Bhar, M. Govender, R. Sharma, *Eur. Phys. J. C* **77**, 109 (2017)
67. M. Kalam, F. Rahaman, S. Monowar Hossein, S. Ray, *Eur. Phys. J. C* **73**, 2409 (2013)
68. M. Hossein, F. Rahaman, J. Naskar, M. Kalam, S. Ray, *Int. J. Mod. Phys. D* **21**, 1250088 (2012)
69. P. Bhar, F. Rahaman, R. Biswas, H.I. Fatima, *Commun. Theor. Phys.* **62**, 221–226 (2014)
70. P. Bhar, *Eur. Phys. J. C* **75**, 123 (2015)
71. P. Bhar, M.H. Murad, N. Pant, *Astrophys. Space Sci.* **359**, 13 (2015)
72. P. Bhar, *Astrophys. Space Sci.* **359**, 41 (2015)
73. P. Bhar, M.H. Murad, *Astrophys. Space Sci.* **361**, 334 (2016)
74. P. Bhar, K.N. Singh, N. Pant, *Indian J. Phys.* **91**(6), 701–709 (2017)
75. P. Bhar, K.N. Singh, T. Manna, *Astrophys. Space Sci.* **361**, 284 (2016)
76. P. Bhar, B.S. Ratanpal, *Astrophys. Space Sci.* **361**, 217 (2016)
77. R. Sharma, B.S. Ratanpal, *Int. J. Mod. Phys. D* **22**, 1350074 (2013)
78. R. Sharma, S.D. Maharaj, *Mon. Not. R. Astron. Soc.* **375**, 1265–1268 (2007)
79. L. Herrera, J. Ospino, A.D. Prisco, *Phys. Rev. D* **77**, 027502 (2008)